LA MÉTROLOGIE AU CŒUR DES TECHNOLOGIES CONTEMPORAINES

Densités de Probabilité du Lag-1 dans les Séries Temporelles Linéaires et Circulaires Modélisant les Processus de Brassage

Probability Densities of Lag-1 in Linear and Circular Time Series Modeling Stirring Processes

Rabah Monsef [1,2]

[1] *Université Paris-Saclay, CentraleSupélec, CNRS, Laboratoire de Génie Electrique et Electronique de Paris (GeePS), 91192 Gif- sur-Yvette, France, rabah.monsef@centralesupelec.fr*
[2] *Sorbonne Université, CNRS, Laboratoire de Génie Electrique et Electronique de Paris, 75252 Paris, France*

Mots clés *: Chambres Réverbérantes, Autocorrélation, Brassage, Électromagnétisme Statistique*
Keywords : Reverberation Chambers, Autocorrelation, Stirring Processes, Statistical Electromagnetism

Résumé/Abstract

Dans les études de chambres réverbérantes, les séries temporelles linéaires (STL) sont traditionnellement utilisées pour modéliser les processus de brassage au sein d'une chambre réverbérante, y compris pour les brasseurs rotatifs. Un travail récent [1] a introduit les séries temporelles circulaires (CTS) comme modèle plus adapté. Cet article complète ce modèle en dérivant la fonction de densité de probabilité (PDF) associée et propose une expression révisée de la PDF mieux adaptée aux brasseurs linéaires. Les expressions proposées améliorent l'accord avec les résultats numériques par rapport aux modèles existants, tout en fournissant un accord satisfaisant pour les modèles circulaires appliqués aux brasseurs rotatifs.

In reverberation chamber studies, linear time series (LTS) have traditionally been used to model stirring processes within a reverberation chamber, including for rotating stirrers. Recent work [1] introduced circular time series (CTS) as a more suitable model. This paper extends the CTS model by deriving the associated probability density function (PDF) and proposes a revised PDF expression better suited for linear stirrers. The proposed expressions improve the agreement with numerical results compared to the expression commonly adopted in the community, while also delivering satisfactory results for circular models applied to rotating stirrers.

1 Introduction

In reverberation chambers (RCs), mechanical stirring ensures field uniformity and isotropy. Field values at each stirrer position are typically modeled using linear time series (LTS), which works well for sliding stirrers but is less suitable for rotating stirrers due to inherent correlations between the first and last positions. Despite this, LTS models remain widely used in the RC community [2-4].

To address this limitation, recent work [1] introduced Circular Time Series (CTS), as a better model for rotating stirrers, though its statistical properties, particularly the PDF of the lag-1 correlation coefficient as a function of stirrer positions referred to as *N*, remain underexplored in the community. This paper addresses this question by deriving the lag-1 PDF for CTS, enabling a rigorous comparison with [5] and studying the influence of N on models' accuracy.

2 Linear and Circular Correlation Models

In the following, we present and recall correlation models when linear and circular time series are considered. Time series apply to a given cartesian components of the electric field in an RC where overmoded conditions are assumed. Real and imaginary parts of the field can be regarded as Gaussian accordingly. For a sake of brevity, we will use variable x to refer to the real or imaginary part of the electric field and subscripts L and C will be used to refer to LTS and CTS models, respectively. Variables x_L and x_C are standardized such that they follow a $N(0, 1)$ law, which is centered and has unit variance.

Regarding autocorrelation models, we use an AR-1 model to describe the relationships between consecutive samples such that,

$$\begin{cases} x_{L_1} = \varepsilon_1 \\ x_{L_2} = \rho x_{L_1} + \alpha_L \varepsilon_2 \\ \vdots \\ x_{L_N} = \rho x_{L_{N-1}} + \alpha_L \varepsilon_N \end{cases}, \tag{1}$$

where $\alpha_L = \sqrt{1-\rho^2}$ and,

$$\begin{cases} x_{C_1} = \rho x_{C_N} + \alpha_c \varepsilon_1 \\ x_{C_2} = \rho x_{C_1} + \alpha_c \varepsilon_2 \\ \vdots \\ x_{C_N} = \rho x_{C_{N-1}} + \alpha_L \varepsilon_N \end{cases}, \tag{2}$$

where $\alpha_c = \alpha_L \sqrt{1-\rho^N/1+\rho^N}$. We can conveniently express (1) and (2) using matrices [1], referred to as $\underline{\boldsymbol{A}}_{LN}$ and $\underline{\boldsymbol{A}}_{CN}$ such that,

$$\underline{\mathbf{A}}_{LN} = \begin{bmatrix} 1 & 0 & 0 & \dots & \dots & 0 \\ \rho & \alpha_l & 0 & \dots & \dots & 0 \\ \rho^2 & \rho\alpha_l & \alpha_l & \dots & \dots & 0 \\ \vdots & \vdots & \vdots & \vdots & \ddots & \vdots \\ \rho^{N-1} & \rho^{N-2}\alpha_l & \rho^{N-3}\alpha_l & \dots & \dots & \alpha_l \end{bmatrix}, \quad \underline{\mathbf{A}}_{CN} = \frac{\alpha_c}{1-\rho^N} \begin{bmatrix} 1 & \rho^{N-1} & \rho^{N-2} & \dots & \rho \\ \rho & 1 & \rho^{N-1} & \dots & \rho^2 \\ \rho^2 & \rho & 1 & \dots & \rho^3 \\ \vdots & \vdots & \vdots & \ddots & \vdots \\ \rho^{N-1} & \rho^{N-2} & \rho^{N-3} & \dots & 1 \end{bmatrix}. \tag{3}$$

These operators allow generating samples based on linear and circular time series such that,

$$\begin{cases} \underline{\mathbf{x}}_L = \underline{\mathbf{A}}_{LN} \underline{\epsilon} \\ \underline{\mathbf{x}}_C = \underline{\mathbf{A}}_{CN} \underline{\epsilon} \end{cases}, \tag{4}$$

where $\underline{\epsilon}$ is a vector of standardized random gaussian variables.

3 Lag-1 Probability Density Distribution

In this section we present three different PDFs expressions for lag-1 correlation coefficient. Explicit expressions of each of them are based on assumptions that urged us computing Monte-Carlo (MC) simulations to evaluate to what extent these expressions hold.

It turns out that the most frequently used PDF in the community is given by [5] such that,

$$\Psi_K(r) = \frac{N-2}{\sqrt{2\pi}} \cdot \frac{\Gamma(N-1)}{\Gamma\left(N-\frac{1}{2}\right)} \frac{(1-\rho^2)^{\frac{(N-1)}{2}} (1-r^2)^{\frac{N-4}{2}}}{(1-\rho r)^{N-\frac{3}{2}}} \left[1 + \frac{1+\rho r}{4(2N-1)} + \dots\right], \tag{5}$$

The reference written in German was not accessible – subsequently we are not aware of the assumptions behind this expression. The derivation of another PDF expression for lag-1 coefficient for LTS can be found in Eq (6-7) of Ref. [6]. In order to have an explicit expression the author has to exclude cases for which ρ is close to ± 1, leading to,

$$\Psi_{l,D} \sim \frac{N}{2\sqrt{\pi}} \frac{\Gamma(\frac{1}{2}N-1)}{\Gamma(\frac{1}{2}N-\frac{1}{2})} \frac{\sqrt{1-\rho^2}\left(1-r^2\right)^{\frac{N}{2}-1}}{(1-\rho r)(1-2\rho r+\rho^2)^{\frac{1}{2}N-1}} (1+O(N^{-1})), \tag{6}$$

Derivation of the PDF for CTS can also be found in [6] although previously derived in [7]. It leads to the following expression given by Eq (3-7) of Ref. [6], such that,

$$\Psi_C(r) \sim \frac{1}{\sqrt{\pi}} \frac{\Gamma(\frac{N}{2}+1)}{\Gamma(\frac{N}{2}+\frac{1}{2})} \frac{(1-r^2)^{\frac{(N-1)}{2}}}{(1-2\rho r+\rho^2)^{\frac{N}{2}}}, \tag{7}$$

where the subscript *C* refers to the circular nature and where the validity domain exclude cases for which ρ is close to ± 1.

4 Monte-Carlo Simulations

Running Monte-Carlo simulations, 25000 realizations were considered using N samples in time series. Fig. 1 shows the numerical PDFs for CTS (squares) and LTS (circles), overlaid with the analytical models given by (5) (solid line), (6) (dotted line) and (7) (dashed line). For low correlation level, i.e., for ρ<0,5, it is interesting to see that none of the models really match MC simulations for a poor number of stirrer positions such as 10. These expressions can be considered as sound for a number of stirrer positions greater than 50 for a 0 to 0.5 range correlation level. Beyond a 0.5-correlation level we can observe that (5) gives the worst match even for the largest number of 200 of stirrer positions considered herein. For the other expressions, two things can be observed. First, they behave (quite surprisingly) the same way, and, second, they match numerical results for N greater than 100. This computations allow pointing out conditions under which these expressions hold.

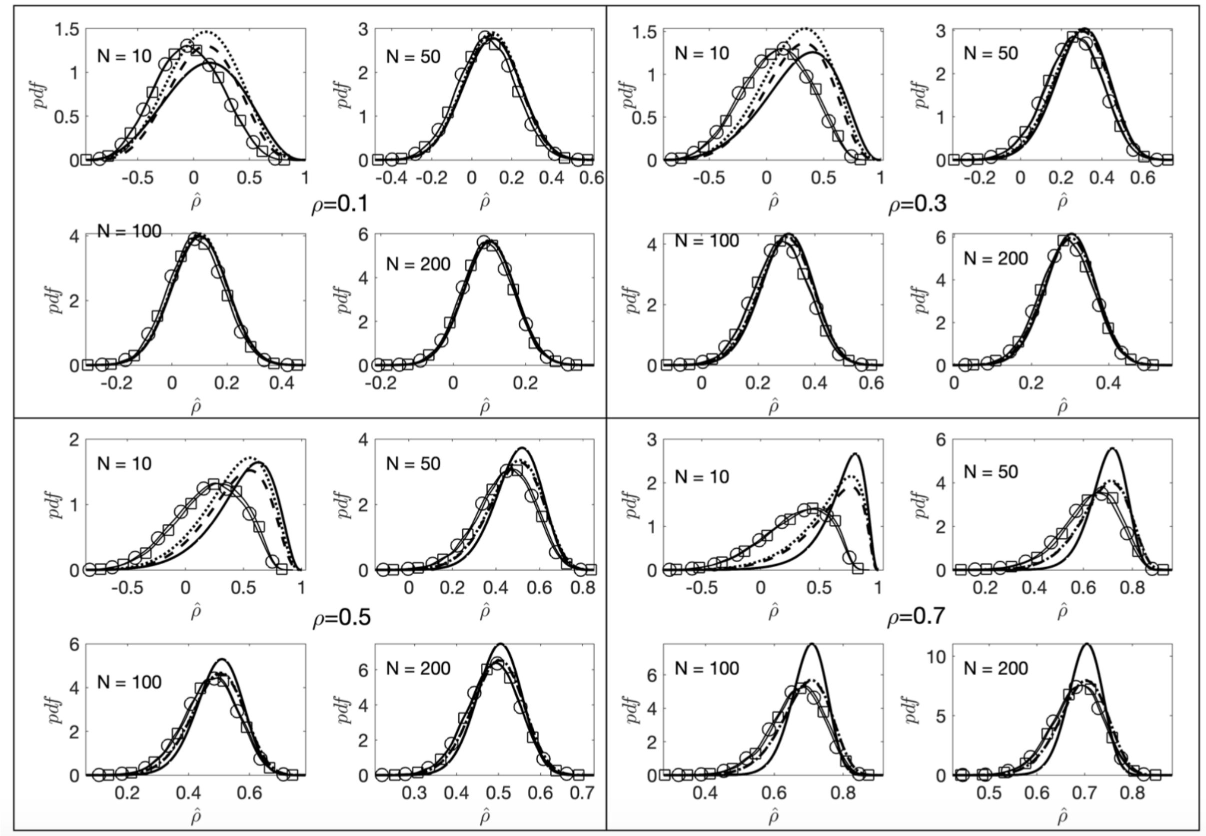

Figure 1: Numerical PDF for CTS (squares) and LTS (circles) with analytical models overlaid ((5)(solid line), (6) (dashed line) and (7) (dotted line)). Four correlation levels have been considered and the number of stirring states is reported in the inset of each case.

Additionally, it is worth remembering that the lags considered here are at the field level, as explained in [9]. When comparing with thresholds provided by standards [8], the mean values of ρ considered here should be squared, meaning that 70% correlation corresponds to less than 50% correlation at the power level.

5 Conclusion

In this work, we derived and compared PDFs for the lag-1 correlation coefficient in both linear and circular time series models. The proposed expressions for LTS and CTS show good agreement with numerical results as long as the number of stirrer states is greater than 50 for correlation level lower than 0.5, whereas 100 stirrer states must be considered for a sound use of them for correlation level larger than 0.5. However, both expressions outperform the commonly used model in the community. These findings provide a more accurate framework for estimating confidence intervals for stirring processes in reverberation chambers, for rotating and linear stirrers.

References

[1] R. F. Monsef, "Rotating-stirring process and circular time series," *IEEE Transactions on Electromagnetic Compatibility*, vol. 66, no. 5, pp. 1679–1682, 2024.

[2] C. Lemoine, P. Besnier, and M. Drissi, "Estimating the effective sample size to select independent measurements in a reverberation chamber," *IEEE Transactions on Electromagnetic Compatibility*, vol. 50, no. 2, pp. 227–236, 2008.

[3] C. Lemoine, P. Besnier, *et al.*, "Using autoregressive models to estimate the number of independent samples available with stirrer rotation in reverberation chamber," in *Electromagnetic Compatibility, 2007. EMC Zurich 2007. 18th International Zurich Symposium on*, IEEE, 2007, pp. 469–472.

[4] A. Reis, F. Sarrazin, E. Richalot, S. Meric, J. Sol, P. Pouliguen, and P. Besnier, "Radar cross-section pattern measurements in a mode-stirred reverberation chamber: Theory and experiments," *IEEE Transactions on Antennas and Propagation*, 2021.

[5] H. G. Krauthauser, T Winzerling, and J. Nitsch, "Statistical interpretation of autocorrelation coefficients for fields in mode-stirred chambers," in *Electromagnetic Compatibility, 2005. EMC 2005. 2005 International Symposium on*, IEEE, vol. 2, 2005, pp. 550–555.

[6] H. Daniels, "The approximate distribution of serial correlation coefficients," *Biometrika*, vol. 43, no. 1/2, pp. 169–185, 1956.

[7] R. Leipnik, "Distribution of the serial correlation coefficient in a circularly correlated universe," *The Annals of Mathematical Statistics*, vol. 18, no. 1, pp. 80–87, 1947. [Online]. Available: https://www.jstor.org/stable/2236104.

[8] *Reverberation Chamber Test Methods*, International Electrotechnical Commission (IEC), Std. 61 000-4-21, 2011.

[9] F. Monsef, A. Cozza, and R. Serra, "Linking lag-1 correlation coefficients between field-related quantities in a reverberation chamber," *IEEE Transactions on Electromagnetic Compatibility*, 2019. DOI: 10.1109/TEMC.2019.2928177.